

Keywords: fuel injector; injector needle; needle profile; de Laval nozzle; fuel consumption; exhaust emissions; engine efficiency; fuel turbulence; fuel injection

Oleh KLYUS¹, Marcin SZCZEPANEK^{2*}, Sławomir OLSZOWSKI³, Barbara ŻURAŃSKA⁴, Leszek CHYBOWSKI⁵

MODIFICATION OF THE FUEL INJECTOR NEEDLE AS A MEANS OF IMPROVING THE ECOLOGICAL AND ECONOMIC PERFORMANCE PARAMETERS OF OLDER-GENERATION COMPRESSION IGNITION ENGINES

Summary. This article investigates how modifications to the geometry of the injector flow channel influence the characteristics of fuel atomization, with particular emphasis on changes in the droplet size distribution. The modification consisted of mechanically forming two toroidal de Laval constrictions in the non-active section of the needle, creating the design variant referred to as 2L. The intention behind this approach was to enhance fuel turbulence within the flow region. The assessment was carried out using a three-hole HILMK 148/1 atomizer equipped with orifices with a 0.34-mm diameter. Experimental tests were performed for the original, unmodified needle as well as for three needles incorporating the above-mentioned structural alterations. All configurations were evaluated during the operation of an older-generation FSC Starachowice S359M compression-ignition engine. The comparative analysis covered a range of parameters describing engine operating conditions and the composition of the resulting exhaust gases. The evaluated indicators included effective power output, mass-based and specific fuel consumption, nitrogen oxides, carbon dioxide and carbon monoxide emissions, exhaust smoke levels, oxygen concentration in the exhaust stream, and overall engine efficiency. The results demonstrate that incorporating the 2L constrictions improves the atomization process, leading to reduced fuel consumption and a measurable decline in carbon dioxide and toxic pollutant emissions. This confirms that the applied needle modification can be an effective means of improving the operational performance of the investigated engine.

1. INTRODUCTION

On July 30, 2024, there were 8,128,527 passenger cars and 3,713,217 diesel-powered trucks registered in Poland. These vehicles had an average mileage of approximately 253,500 km and an average age of 16 years [1]. These figures indicate that the strict emission standards for toxic compounds in exhaust gases (EG) defined by EURO V, EURO VI, or TIER III regulations are not met by

¹ Maritime University of Szczecin, Faculty of Marine Engineering; Willowa 2, 71-650 Szczecin, Poland; e-mail: o.klyus@pm.szczecin.pl; orcid.org/0000-0002-9849-5974

² Maritime University of Szczecin, Faculty of Marine Engineering; Willowa 2, 71-650 Szczecin, Poland; e-mail: m.szczepanek@pm.szczecin.pl; orcid.org/0000-0002-0764-9772

³ Casimir Pulaski Radom University, Faculty of Transport, Electrical Engineering and Computer Science; J. Malczewskiego 29, 26-600 Radom, Poland; e-mail: s.olszowski@uthrad.pl; orcid.org/0000-0001-5991-9124

⁴ Maritime University of Szczecin, Faculty of Marine Engineering; Willowa 2, 71-650 Szczecin, Poland; e-mail: b.zuranska@pm.szczecin.pl; orcid.org/0009-0004-7067-4227

⁵ Maritime University of Szczecin, Faculty of Marine Engineering; Willowa 2, 71-650 Szczecin, Poland; e-mail: l.chybowski@pm.szczecin.pl; orcid.org/0000-0003-0245-3946

* Corresponding author. E-mail: m.szczepanek@pm.szczecin.pl

the majority of vehicles, even though they comply with emission norms tested during periodic inspections at vehicle inspection stations.

Internal combustion engines continue to be the primary type of propulsion in land and marine transport, as well as for powering stationary equipment. Research is being conducted to reduce the negative environmental impact of engines by improving their efficiency, which leads to lower fuel consumption (and consequently reduced use of fossil fuels), decreased emissions of greenhouse gases—primarily carbon dioxide (CO₂) and nitrous oxide (N₂O) in engine exhaust—and reduced levels of toxic substances in the exhaust gases, including nitrogen oxides (NO_x), carbon monoxide (CO), hydrocarbons and particulate matter) [2–4]. One of the methods for improving engine efficiency and reducing its environmental impact is the modification of the combustion processes.

The quality of the combustion process depends on many factors, including fuel preparation before its delivery to the cylinder [5, 6]. Optimizing these processes can improve engine efficiency and reduce the emission of harmful substances in the EG. When fuel is injected into the cylinder of an internal combustion engine, cavitation phenomena occur inside the injector [7, 8]. These phenomena adversely affect the injector components, leading to nozzle wear [9–12]. At the same time, increased turbulence within the fuel stream delivered to the cylinder intensifies the atomization of the fuel into droplets and accelerates the formation of a homogeneous combustible mixture with the desired parameters [13]. The disintegration of the injected fuel stream is further intensified by the formation of gas bubbles under cavitating flow conditions [14].

The formation of vortices and cavitation bubbles is a complex process influenced by various factors, including the shape of the channels through which the fuel flows inside the nozzle [15, 16]. The modification of the flow channel geometry within the injector, specifically on the injector needle, has been the subject of previous studies [7, 8, 17]. Depending on the shape of the nozzle outlet channel and the flow conditions, vortices can form in the fuel stream; these are directly related to the air-fuel mixture formation process inside the cylinder [18]. A modification of the fuel injector nozzle does not require highly skilled personnel and can be done at any stage of the engine's service life.

Drawing on the findings of the study, patented injector designs were formulated that enhance fuel turbulence within the atomizer nozzle (Patent 205428) and the use of a de Laval nozzle on the passive surface of the injector needle (Patent 239493). One of these concepts was implemented using the H1LMK148/1 fuel injector (also designated D1LMK148/1) for which prototypes equipped with needles featuring toroidal de Laval nozzles were created. The effect of needle profile modification on fuel atomization quality was examined.

The fuel spray generated by this injector was subjected to granulometric analysis. For this purpose, the laser diffraction method using a Malvern Spraytec STP 500 device was applied to assess the droplet size and the distribution characteristics of the fuel spray produced by the tested injector units [19]. Comparative tests were conducted for an injector with the original (unmodified) needle and injectors with modified needle profiles. The modified needle versions, marked with the signatures 1L, 2L, and 3L, were distinguished by the presence of one, two, and three toroidal nozzles, respectively, machined into the passive surface of the injector needle (Fig. 1).

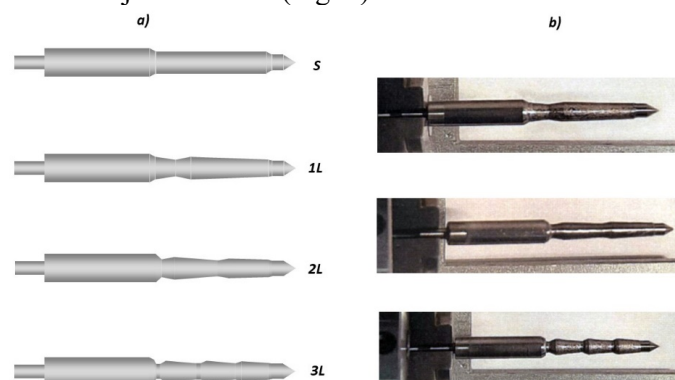


Fig. 1. H1LMK 148/1 injector needles [20]: (a) profiles applied in the experiment and (b) images of a representative specimen

The results of the droplet diameter profile measurements imply that the use of atomizers with a modification to the internal flow channel of the injector (modified contour surface of the needle) increases the share of smaller-diameter droplets compared to the standard nozzle. At the same time, the 2L atomizer needle demonstrated the most stable atomization behavior. A comparison of the average values of the granulometric droplet diameter distribution for the tested atomizers is presented in Fig. 2.

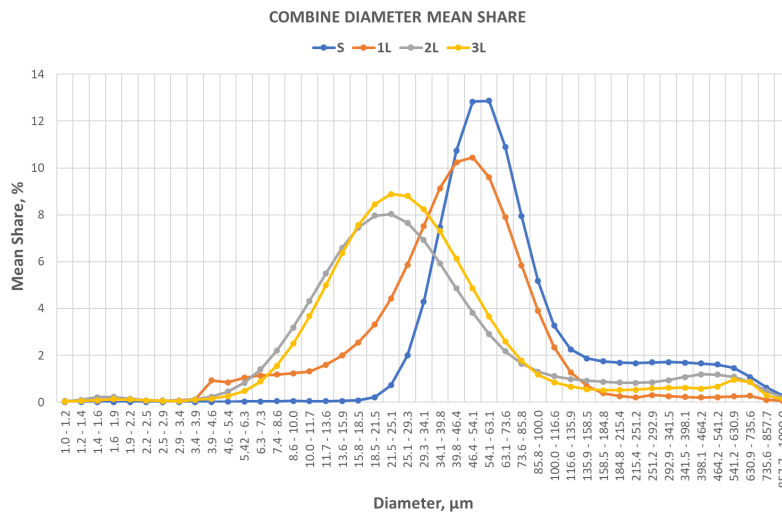


Fig. 2. Average granulometric parameters of the fuel droplet size distribution for each injector needle configuration [21]

The authors concluded that the next step is to conduct further research to assess the impact of modifying the passive surface profile of the injector needle on the engine's economic and environmental performance indicators. As a result of subsequent actions, this plan has been initially implemented. An active experiment was conducted on an engine test bench; its results are presented in the following section.

2. MATERIALS AND METHODS

2.1. Test Bench

The experimental work was conducted on an engine test bench whose schematic layout is presented in Fig. 3. The central element of the bench is a brake system that allows continuous and precise load adjustment. For this study, a hydraulic dynamometer brake (21) of the HH-3 type was employed. The unit is equipped with a bidirectional electric motor enabling the smooth regulation of the load imposed on the tested internal combustion engine (6).

The brake incorporates a dial-type dynamometer (12), which provides a direct reading of the applied load force P [kG]. Using these readings along with appropriate computational procedures makes it possible to determine the torque and effective power characteristics of the engine across a broad spectrum of engine speeds.

On one side, the hydraulic brake is indirectly connected to the crankshaft of the tested engine via the drive shaft (18), which transmits the engine's torque to the brake. The engine speed of the tested engines was measured using a DT-1236L optical-contact laser tachometer, which allows for non-contact measurement of rotating components. This tachometer can measure engine speeds in the range of 0 to $19,999 \text{ min}^{-1}$ with an accuracy of: $0...999.9 \pm 0.1 \text{ min}^{-1}$; $1,000...19,999 \pm 1 \text{ min}^{-1}$.

An absorptive smoke meter of type DS2 in the EcoEuroGreen version was used to measure the smoke opacity coefficient during the tests. A portable analyzer (Testo 350 Maritime) was used to determine the composition of the EG; its key technical parameters are listed in Table 1. Sampling was

performed with a dedicated probe that allows quick and straightforward installation. Concentrations of NO_x, CO, CO₂, oxygen (O₂), and sulfur dioxide (SO₂) were measured using certified electrochemical sensors characterized by high accuracy and long-term operational stability. CO₂ content was determined using a certified infrared (IR) measurement system.

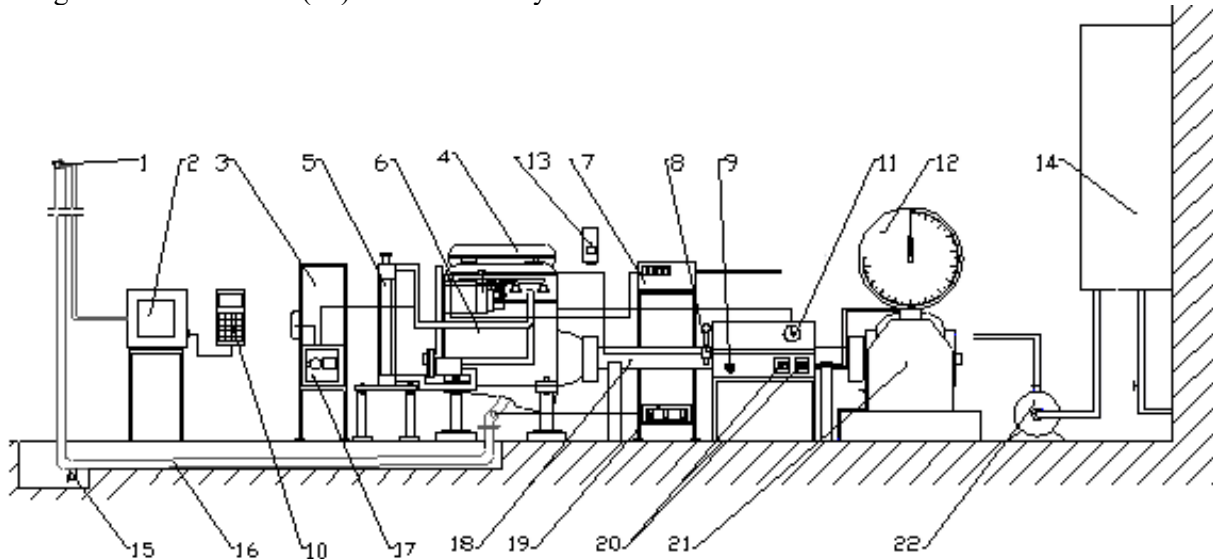


Fig. 3. Diagram of the engine test bench for tested engines and fuel types: 1 – exhaust gas sampling probe for the smoke meter, 2 – DS2 smoke meter in EcoEuroGreen (PC-W64) version and Testo 350 Maritime exhaust gas analyzer, 3 – axial blade fan, 4 – engine air filter, 5 – engine radiator, 6 – tested S359M engine, 7 – mass fuel consumption meter, 8 – engine speed control lever, 9 – starter switch, 10 – exhaust gas analyzer control panel, 11 – dial-type engine temperature indicator, 12 – hydraulic brake dynamometer, 13 – DT-1236L optical-contact laser tachometer, 14 – brake fluid supply tank (HH-3), 15 – engine exhaust system drain valve, 16 – exhaust outlet pipe, 17 – engine temperature control device, 18 – drive shaft, 20 – smooth-load engine control switches, 21 – hydraulic brake type HH-3, 22 – brake supply pump

Table 1

Exhaust gas analyzer measuring ranges [22]

Measuring range		Tolerance
°C, exhaust gas	-40 to +1000 °C	max. ±5 K
O ₂	0 to 25 Vol. %	
CO	0 to 3000 ppm	
NO	0 to 3000 ppm	According to MARPOL Annex VI
NO ₂	0 to 500 ppm	NO _x Technical Cod
SO ₂	0 to 3000 ppm	
CO ₂ (IR)	0 to 40 Vol. %	
P _{abs}	600 to 1150 hPa	±5 hPa at +22 °C ±10 hPa at -5 to +45 °C

Fuel usage was assessed with a gravimetric fuel-measuring unit (7) integrated into the engines' fuel supply line between the tanks and the fuel filter. The instrument determines the elapsed time required to consume a constant fuel mass of 42 g, operating over a range of 0–999.9 s with a precision of 0.1 s.

2.2. Tested Engine and Injectors

In line with the idea of improving the ecological and energy performance parameters of older-generation compression ignition engines, the bench tests were conducted on a six-cylinder S359M engine with direct fuel injection, which is commonly used in STAR-type heavy-duty vehicles. Table 2 provides the parameters of the tested engine.

Table 2

Engine Parameters S359M [23]

Type of fuel	Diesel
Engine design	In-line engine
Number of cylinders	6
Firing order	1 – 5 – 3 – 6 – 2 – 4
Cylinder bore	110 mm
Piston stroke	120 mm
Cubic capacity	6,842 dm ³
Compression ratio	17
Rated power	
Rated speed	
Maximum engine speed	3100 rpm
Maximum torque	432 Nm
Engine speed at maximum torque	1800÷2100 rpm
Minimum specific fuel consumption	218 g/kWh
Specific fuel consumption at rated power	248 g/kWh
Static injection advance angle before TDC	18±1 ⁰
Injection pressure	22 ⁺¹ MPa
Rated injection pump delivery	65 mm ³ /injection

The studied engine was equipped with a 3-hole fuel injector H1LMK148/1 (PZL-WZM, Jawczyce, Poland) [17]. The dimensions of the injector nozzle are presented in Table 3. A cross-sectional view and the hole arrangement of the atomizer are shown in Fig. 4.

Table 3

Characteristics of the oil-mist spray and geometrical parameters of the atomizer [24]

The geometry of the atomizer slot	
Diameter of the atomizer orifice d_0	0.34 mm
Length of the atomizer channel l_0	1.2 mm
Length-to-diameter ratio of the atomizer channel l_0/d_0	3.53
Number of atomizer orifices	3

The tests were conducted using standard (original) version injectors and a modified version designated with the code 2L. The modified needle version features a machined passive surface designed to form two toroidal de Laval nozzles. The engine bench tests were carried out using hydrocarbon fuel compliant with PN-EN 590 [25], as recommended by the engine manufacturer. The engine is equipped with a P76-G103u06110VR type injection pump and W1F01 injectors with D1LMK 148/1 nozzles [16].

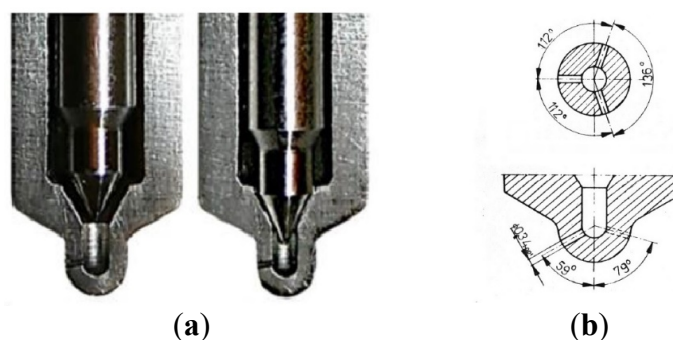


Fig. 4. The H1LMK148/1 atomizer [26]: (a) cross-section in the open (left) and closed (right) positions; (b) dimensions and locations of openings in the atomizer nozzle

2.3. Test Plan and Conditions

The tests were conducted at a fixed engine load of approximately 40 Nm, applied using the dynamometer brake. Under these conditions, selected engine operating parameters were measured at fixed engine speeds of 100, 1200, 1800, 2000, 2400, and 2800 rpm. All measurements were performed under comparable ambient conditions for the engine equipped with both the original and the modified version of the injector. The differences in ambient conditions are presented in Table 4.

Table 4

Ambient conditions during the experiment

Parameter	Engine with standard injector	Engine with modified injector (2L)
Ambient temperature	23.0°C	21.0°C
Atmospheric pressure	1000 hPa	1020 hPa
Relative air humidity	43%	35%

For each load condition, the engine's effective power was determined based on the measured torque and engine speed. Simultaneously, the mass fuel consumption and exhaust gas composition were measured. The emission of individual exhaust components was determined using a TESTO analyzer for measuring nitrogen oxides (NO_x), carbon dioxide (CO₂), and oxygen (O₂) content in the EG, as well as a smoke meter for measuring exhaust smoke opacity. Additionally, the specific fuel oil consumption and overall engine efficiency were calculated based on the calculated power and the measured mass fuel flow over time.

Due to variability in some parameters (owing to the operating characteristics of the single-cylinder engine), exhaust gas composition and energy indicators were compared with reference to the maximum, minimum, and average values obtained across the entire analyzed engine load range. As the experiment represents the preliminary phase of the bench investigations, the authors assumed that the applied scope of analysis is adequate for an initial assessment of how the proposed injector-needle geometry modification influences the energy performance and emission characteristics of an internal combustion engine fitted with the altered injectors.

2.4. General engine performance

The effective engine power for all analyzed load conditions is presented in Fig. 5. Under steady-state conditions with a constant load torque T , the engine output power P_e increases proportionally with the engine speed n according to the following formula:

$$P_e \text{ [kW]} = \frac{\pi \cdot n \cdot T \text{ [Nm]}}{3000} \quad (1)$$

Similar values are obtained for both injector versions, and the maximum differences in effective power are observed at 2400 rpm, where the power output of the engine equipped with the modified injector is approximately 15 kW higher than that of the engine with the standard injector.

These differences can be explained by the influence of the speed control system and the operation of the brake, whose characteristics are never linear. In Fig. 5, linear function models have been plotted for the collected empirical data describing the engine load conditions. The figure also includes the mathematical description of these models and their goodness of fit expressed by the coefficient of determination R^2 , which for both data sets is $R^2 > 0.99$, indicating a very good fit of the presented models to the empirical data.

Additionally, differences may result from improved combustion conditions due to better fuel atomization in the cylinder of the engine equipped with the modified injector. This is associated with a shorter ignition delay and reduced combustion duration. This effect is confirmed by the reduction in fuel consumption, shown in Fig. 6.

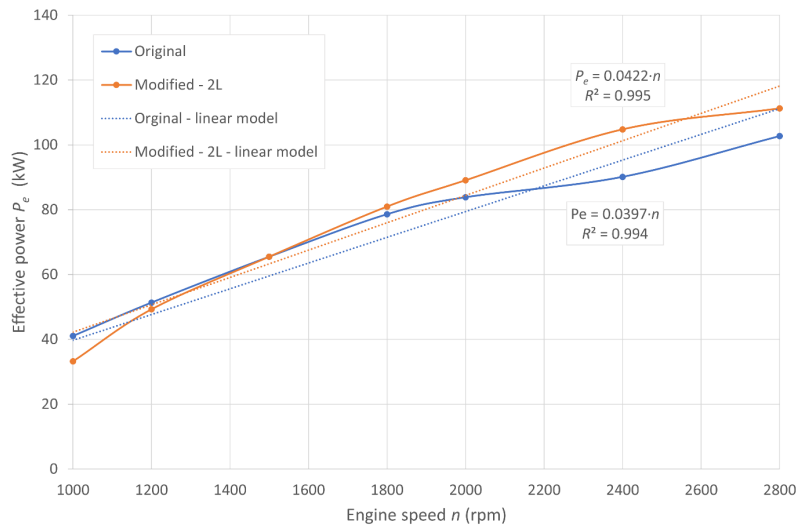


Fig. 5. Engine mass fuel-consumption characteristic as a function of engine speed

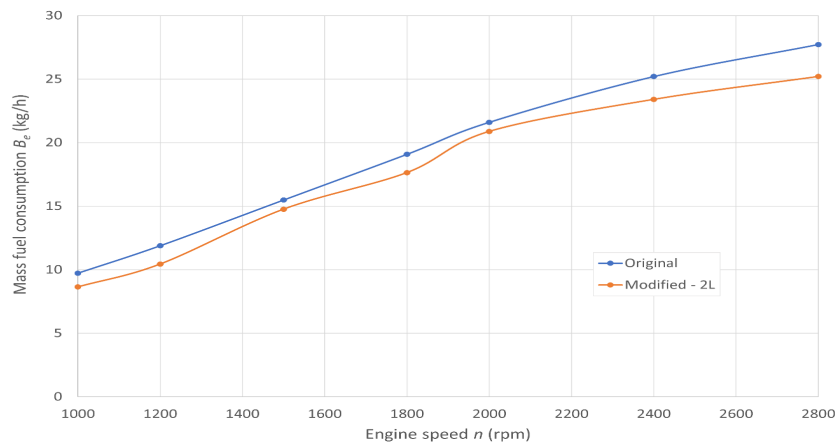


Fig. 6. Hourly mass fuel-consumption characteristic of the tested engine as a function of engine speed

Across all examined load settings, the engine fitted with the modified injector exhibited lower time-based mass fuel consumption than the unit operating with the standard injector. The measured reductions ranged from 0.72 to 2.52 kg/h, which corresponds to an approximate decrease of 12.13% relative to the baseline configuration. This outcome aligns with the tendencies previously reported in earlier research [27, 28].

3. RESULTS AND DISCUSSION

3.1. Exhaust gas composition

The values of NO_x emissions in the EG obtained during the experiment are presented in Fig. 7. Across the entire load range, the NO_x emission level for the engine equipped with the modified fuel injector was slightly lower than that of the engine with the standard injector. The maximum, average, and minimum NO_x emission levels were lower by 7, approximately 12, and 8 ppm, respectively. For the presented case, these differences are negligible, as the relative percentage difference compared to the reference value (standard injector) is approximately 1.4%.

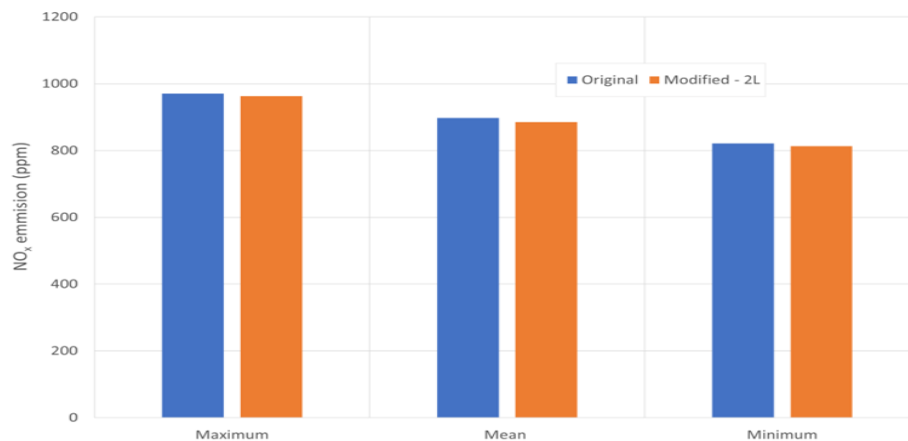


Fig. 7. Recorded NOx emission levels in the EG of the engine equipped with the tested injectors

The CO₂ emission values obtained during the experiment are presented in Fig. 8. The maximum CO₂ emission level for the engine equipped with the modified fuel injector was slightly higher (by 0.63% v/v) than that of the engine with the standard injector.

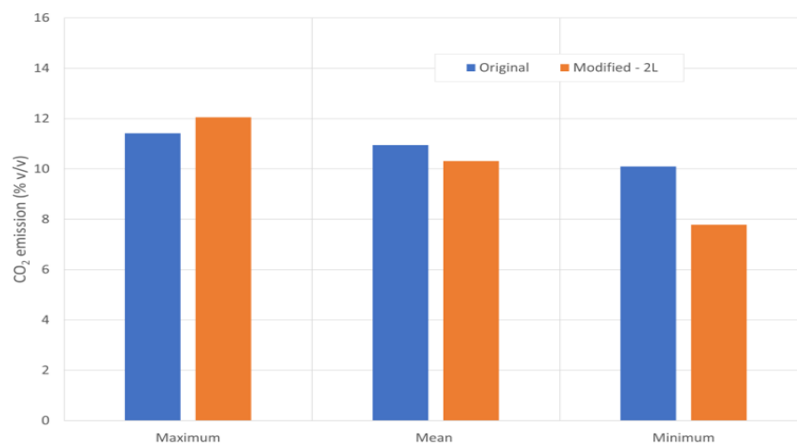


Fig. 8. Recorded CO₂ emission levels in the EG of the engine equipped with the tested injectors

The average and minimum CO₂ emission values were lower for the modified injector than the standard injector by 0.63% v/v and 2.32% v/v, respectively. With respect to the average value, the relative percentage difference compared to the reference value (standard injector) is approximately 5.8%, owing to the reduction in fuel consumption. The results concerning the potential reduction in CO₂ emission levels are consistent with assumptions previously presented by the authors [21].

The CO emission values obtained during the experiment are presented in Fig. 9. The minimum emission levels are similar for both injectors, at approximately 1000 ppm. Meanwhile, the maximum and average CO emission levels for the engine equipped with the modified fuel injector were significantly lower than those for the engine with the standard injector by 1022 ppm and approximately 520 ppm, respectively.

With respect to the average value, the relative percentage difference compared to the reference value (standard injector) is approximately 15.5%, which is likely due to improved combustion conditions and reduced fuel consumption.

Fig. 10 presents the oxygen concentration in the exhaust gases generated by the engine during the experiment. The maximum and average values are higher for the engine equipped with the modified injector, while the minimum value is higher for the unmodified injector. For both injectors, the differences in average and minimum values are small (< 1% v/v).

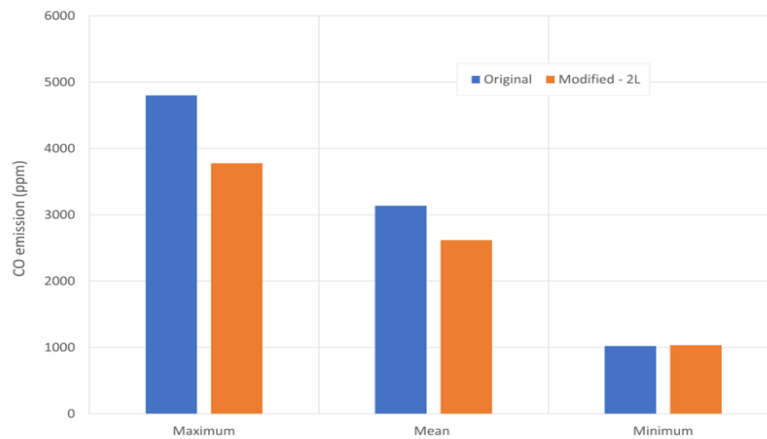


Fig. 9. CO emission values detected in the EG of the engine equipped with the evaluated injectors

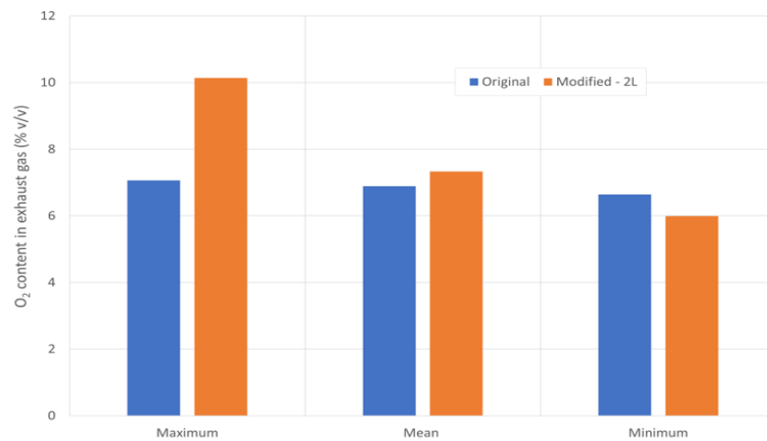


Fig. 10. Recorded oxygen levels in the exhaust stream for the engine equipped with the tested injector variants

The exhaust smoke opacity generated by the engine during the experiment is presented in Fig. 11. The maximum, average, and minimum values are lower for the engine equipped with the modified injector than for that equipped with the unmodified injector.

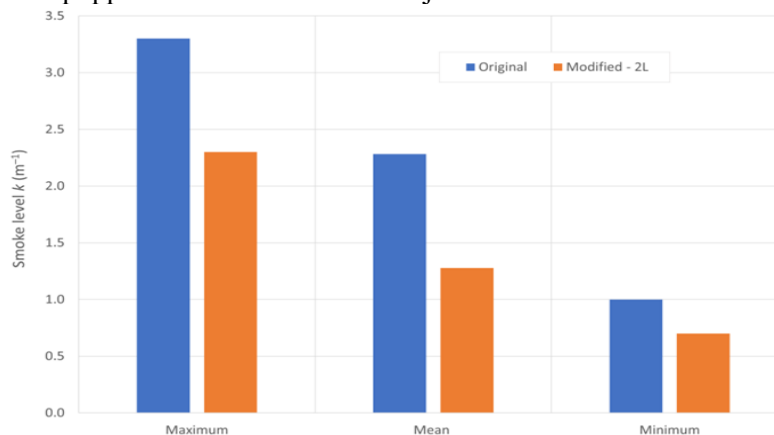


Fig. 11. Recorded exhaust smoke opacity emitted by the engine equipped with the tested injectors

The differences in the maximum, average, and minimum values of the coefficient of light absorption are $1 m^{-1}$, $1 m^{-1}$, and $0.3 m^{-1}$, respectively. The results suggest improved combustion efficiency. For the presented case, these differences are significant, as the relative percentage difference in the average value compared to the reference value (standard injector) is approximately 44%.

3.2. Energetic effectiveness

The specific fuel oil consumption was calculated based on the recorded values of the engine's effective power and time-based mass fuel consumption. The maximum, average, and minimum values for the engine equipped with each of the tested injectors are presented in Fig. 12.

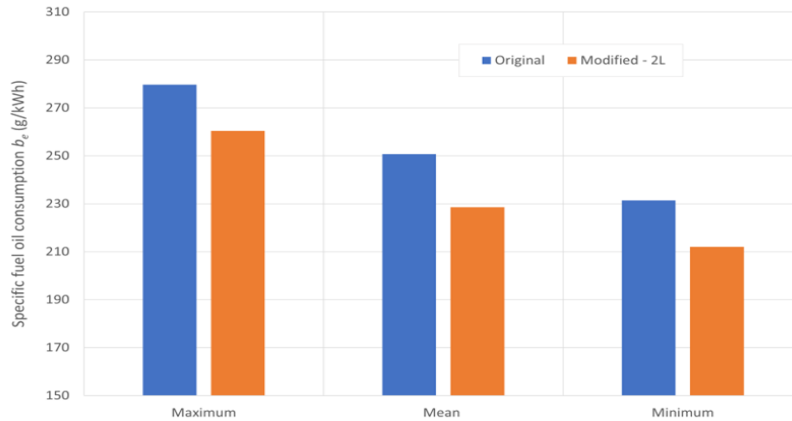


Fig. 12. Specific fuel oil consumption of the engine equipped with the tested injectors

The values obtained for the engine with the modified injector are lower than those for the engine with the standard injector. The differences in the maximum, average, and minimum specific fuel oil consumption are approximately 26.6, 22.1, and 19.4 g/kWh, respectively. For the presented case, these differences are significant, as the relative percentage difference in the average value compared to the reference value (standard injector) exceeds 8.8%. This effect aligns with expectations outlined by the authors in previous studies [21].

Based on the calculated specific fuel oil consumption values and the estimated lower heating value of the fuel ($\sim 41,234.7$ kJ/kg), the overall efficiency of the engine under the given operating conditions was calculated for both the standard and modified injector configurations. The resulting engine efficiency values are shown in Fig. 13.

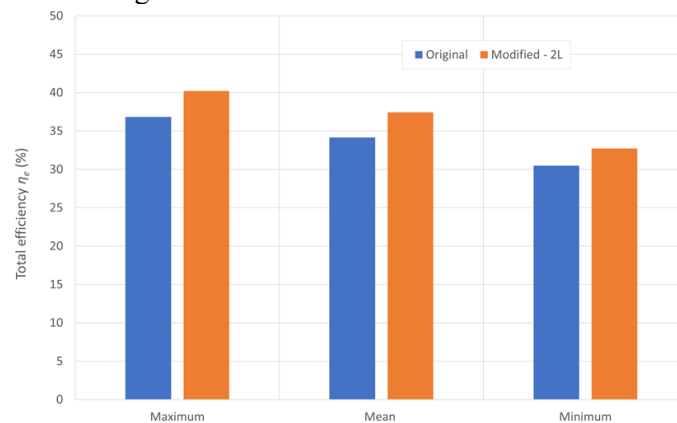


Fig. 13. Overall efficiency of the engine equipped with the tested injectors

As expected, and as indicated in the authors' previous studies [21], the maximum, average, and minimum values of overall efficiency calculated for the tested range of engine loads and operating conditions were higher by approximately 2.2–3.4% for the engine equipped with the modified injector. In the presented case, these differences are significant, as the relative percentage difference in average overall efficiency compared to the reference value (standard injector) is approximately 9.6% of the efficiency value for the engine with the unmodified injector.

4. CONCLUSIONS

The experimental program and subsequent analytical procedures substantiate the formulation of the following conclusions:

- 1) The proposed modifications to the nozzle needle design can be implemented under industrial conditions. The shaping of the passive section of the needle in the form of toroidal de Laval nozzles can be applied to newly manufactured components intended for original equipment (OE) installation. It can also be adapted for use in the independent aftermarket.
- 2) The advantage of this concept extends beyond the modernization and optimization of newly manufactured components, as it also offers the opportunity to improve the quality of replacement parts used during inspections and maintenance activities.
- 3) Importantly, these modifications can also be implemented in injectors installed in vehicles already in operation by using upgraded components during repair processes. This creates tangible societal benefits, as vehicles currently in use, which represent the vast majority of the fleet, can be serviced with technologically advanced parts, leading to improved engine efficiency and a reduction in toxic exhaust emissions on a large scale.
- 4) The obtained operational parameters of the engine, such as specific fuel consumption and overall efficiency, indicate improved fuel economy in the engine equipped with modified fuel injectors. An engine fitted with a complete injection system using needles shaped like dual de Laval nozzles demonstrated an 8.8% improvement in specific fuel oil consumption (average relative percentage difference compared to the reference value), which contributed to a 3.3% increase in overall efficiency.
- 5) The environmental performance results obtained for the engine with modified injectors are promising. Compared to the reference injector, the average relative percentage reduction in exhaust opacity for the modified injector was approximately 44%. Meanwhile, carbon monoxide emissions decreased by ~15.5%, carbon dioxide emissions decreased by ~5.8%, and nitrogen oxide emissions decreased by ~1.4%.

The current results support the value of efforts aimed at improving the economic and environmental performance indicators of compression-ignition engines through nozzle needle modification. They also allow for the formulation of a practical conclusion regarding the potential application of the developed design solutions in the context of reducing the negative environmental impact of combustion-based transport. The effectiveness of pro-environmental actions should not be limited to the implementation of strict exhaust emission standards for newly manufactured vehicles with piston engines but should also include vehicles already in operation. Solutions that can be implemented within the aftermarket may play a significant role in this regard. Their design, which is based on scientifically verified premises, reduces harmful exhaust emissions and improves the overall energy efficiency of engines. The technical feasibility of implementing the proposed modifications in existing fuel systems enables their wide application without the need to alter engine architecture, making them an attractive tool that supports sustainable transport policies.

Further studies may involve an in-depth theoretical analysis of fuel flow phenomena within injector channels and the resulting impact of channel shape modifications inside the nozzle on the engine's energy performance indicators.

References

1. *Pojazdy zarejestrowane w 2025 roku*. 2025. Available at: <https://www.gov.pl/web/cepik/pojazdy-zarejestrowane-w-2025-roku>. [In Polish: *Vehicles registered in 2025*].
2. Sahoo, B.B. & Sahoo, N. & Saha, U.K. Effect of engine parameters and type of gaseous fuel on the performance of dual-fuel gas diesel engines—A critical review. *Renewable and Sustainable Energy Reviews*. 2009. Vol. 13. P. 1151-1184. DOI: 10.1016/j.rser.2008.08.003.

3. Heywood, J.B. *Internal combustion engine fundamentals*. New York: McGraw-Hill Education. 2018.
4. Singh, P. & Kumar, R. & Sharma, S. & Kumar, S. Effect of Engine Parameters on the Performance of Dual-Fuel CI Engines with Producer Gas – A Review. *Energy & Fuels*. 2021. Vol. 35. P. 16377-16402. DOI: 10.1021/acs.energyfuels.1c02279.
5. Burgoyne, J. & Cohen, L. The effect of drop size on flame propagation in liquid aerosols. *Proceedings of the Royal Society A*. 1954. Vol. 225. P. 375-392. DOI: 10.1098/rspa.1954.0210.
6. Abderrezzak, B. & Huang, Y. A contribution to the understanding of cavitation effects on droplet formation through a quantitative observation on breakup of liquid jet. *International Journal of Hydrogen Energy*. 2016. Vol. 41. P. 15821-15828. DOI: 10.1016/j.ijhydene.2016.04.209.
7. Badock, C. & Wirth, R. & Fath, A. & Leipertz, A. Investigation of cavitation in real size diesel injection nozzles. *International Journal of Heat and Fluid Flow*. 1999. Vol. 20. P. 538-544. DOI: 10.1016/S0142-727X(99)00043-0.
8. Aleiferis, P.G. & Papadopoulos, N. Heat and mass transfer effects in the nozzle of a fuel injector from the start of needle lift to after the end of injection in the presence of fuel dribble and air entrainment. *International Journal of Heat and Mass Transfer*. 2021. Vol. 165. No. 120576. DOI: 10.1016/j.ijheatmasstransfer.2020.120576.
9. Olszowski, S. Ecological and functional aspect of technical exploitation of new generation common Rail systems. In: *Computer Systems Aided Science and Engineering Work in Transport, Mechanics and Electrical Engineering*. Kazimierz Pulaski Technical University of Radom: Faculty of Transport. 2008. P. 459-465.
10. Olszowski, S. The present and long-term technical problems of exploitation of technologically advanced direct injection diesel systems. *Problems of Mechanics*. 2013.
11. Elamin, F. & Gu, F. & Ball, A. Diesel Engine Injector Faults Detection Using Acoustic Emissions Technique. *Modern Applied Science*. 2010. Vol. 4(9). P. 3-13. DOI: 10.5539/mas.v4n9p3.
12. Gharib, H. & Kovács, G. A Review of Prognostic and Health Management (PHM) Methods and Limitations for Marine Diesel Engines: New Research Directions. *Machines*. 2023. Vol. 11. No. 695. DOI: 10.3390/machines11070695.
13. Salvador, F.J. & Martínez-López, J. & Romero, J-V. & Roselló, M-D. Computational study of the cavitation phenomenon and its interaction with the turbulence developed in diesel injector nozzles by Large Eddy Simulation (LES). *Mathematical and Computer Modelling*. 2013. Vol. 57. P. 1656-1662. DOI: 10.1016/j.mcm.2011.10.050.
14. Dai, X. & Wang, Z. & Liu, F. & Lee, C-F. et al. The effect of bubbles on primary breakup of diesel spray. *Fuel*. 2020. Vol. 263. No. 116664. DOI: 10.1016/j.fuel.2019.116664.
15. Mitroglou, N. & Stamboliyski, V. & Karathanassis, I.K. et al. Cloud cavitation vortex shedding inside an injector nozzle. *Experimental Thermal and Fluid Science*. 2017. Vol. 84. P. 179-189. DOI: 10.1016/j.expthermflusci.2017.02.011.
16. Mitroglou, N. & McLorn, M. & Gavaises, M. et al. Instantaneous and ensemble average cavitation structures in Diesel micro-channel flow orifices. *Fuel*. 2014. Vol. 116. P. 736-742. DOI: 10.1016/j.fuel.2013.08.060.
17. Sa, B. & Markov, V. & Kamaltdinov, V. A numerical study of the effect of spiral counter grooves on a needle on flow turbulence in a diesel injector. *Fuel*. 2021. Vol. 290. No. 120013. DOI: 10.1016/j.fuel.2020.120013.
18. Gomez Santos, E. & Shi, J. & Gavaises, M. et al. Investigation of cavitation and air entrainment during pilot injection in real-size multi-hole diesel nozzles. *Fuel*. 2020. Vol. 263. No. 116746. DOI: 10.1016/j.fuel.2019.116746.
19. Markov, V. & Sa, B. & Kamaltdinov, V. et al. Investigation on the effect of the flow passage geometry of diesel injector nozzle on injection process parameters and engine performances. *Energy Science & Engineering*. 2022. Vol. 10. P. 552-577. DOI: 10.1002/ese3.1051.
20. Klyus, O. Simultaneous reduction of fuel consumption and toxic emission of exhaust gases of high speed diesel engines. *International Multidisciplinary Scientific GeoConference SGEM*. 2017. Vol. 17. P. 801-808.

21. Klyus, O. & Szczepanek, M. & Kidacki, G. et al. The effect of internal combustion engine nozzle needle profile on fuel atomization quality. *Energies*. 2024. Vol. 17. No. 266. DOI: 10.3390/EN17010266.
22. *Testo 350 - Analysis Box for exhaust gas analysis systems*. 2025. Available at: <https://www.testo.com/en-UK/testo-350/p/0632-3510>.
23. *STAR 28 SHL A3-573*. 2024. Available at: <https://www.wicarsworld.pl/star/star-28-shl-a3-573/>.
24. Woźniak, J. *Budowa i naprawa samochodów STAR 266 i pochodnych 2066*. Available at: <https://www.wim.wat.edu.pl/wp-content/uploads/2024/01/Star266-Inst.Pneum.pdf>. [In Polish: *Construction and repair of STAR 266 vehicles*].
25. *European Committee for Standardization. EN 590:2022 Automotive fuels - Diesel - Requirements and test methods*. 2022. Available at: <https://www.nationwidefuels.co.uk/fuel-specifications/en-590/>.
26. Chybowski, L. & Szczepanek, M. & Gawdzińska, K. Particles morphology of mechanically generated oil mist mixtures of SAE 40 grade lubricating oil with diesel oil in the context of explosion risk in the crankcase of a marine engine. *Energies*. 2023. Vol. 16. No. 3915. DOI: 10.3390/en16093915.
27. Ni, P. & Xu, H. & Zhang, Z. & Zhang, X. Effect of injector nozzle parameters on fuel consumption and soot emission of two-cylinder diesel engine for vehicle. *Case Studies in Thermal Engineering*. 2022. Vol. 34. No. 101981. DOI: 10.1016/j.csite.2022.101981.
28. Ivanov, V.S. & Frolov, S.M. & Semenov, I.V. et al. Crankcase explosions in marine diesel engines: a computational study of unvented and vented explosions of lubricating oil mist. *Journal of Marine Science and Engineering*. 2023. Vol. 12. No. 82. DOI: 10.3390/jmse12010082.

Received 18.06.2024; accepted in revised form 20.02.2026